Synthesis, Characterization, X-ray crystallography and DNA binding activities of Co(III) and Cu(II) complexes with a pyrimidine-based Schiff base ligand

Rajesh Pradhan, Milon Banik, David B. Cordes, Alexandra M.Z. Slawin, Nitis Chandra Saha

PII: S0020-1693(15)00569-1
DOI: http://dx.doi.org/10.1016/j.ica.2015.11.015
Reference: ICA 16773

To appear in: *Inorganica Chimica Acta*

Received Date: 8 August 2015
Revised Date: 6 November 2015
Accepted Date: 12 November 2015

Please cite this article as: R. Pradhan, M. Banik, D.B. Cordes, A.M.Z. Slawin, N.C. Saha, Synthesis, Characterization, X-ray crystallography and DNA binding activities of Co(III) and Cu(II) complexes with a pyrimidine-based Schiff base ligand, *Inorganica Chimica Acta* (2015), doi: http://dx.doi.org/10.1016/j.ica.2015.11.015

Synthesis, Characterization, X-ray crystallography and DNA binding activities of Co(III) and Cu(II) complexes with a pyrimidine-based Schiff base ligand

Rajesh Pradhan [a], Milon Banik [b], David B. Cordes [c], Alexandra M.Z. Slawin [c], Nitis Chandra Saha [a,*]

[a] *Department of Chemistry, University of Kalyani, Kalyani-741 235, India*

[b] *Department of Biochemistry & Biophysics, University of Kalyani, Kalyani-741 235, India*

[c] *School of Chemistry, University of St Andrews, North Haugh, St Andrews, Fife, KY16 9ST U.K.*

Abstract

A new pyrimidine based 'NNO' tridentate ligand 2,4-dihydroxyacetophenone-4,6-dimethyhydrazino pyrimidine (H_2MH_yP) (complex **I**) has been synthesized and characterized by elemental analyses, mass, IR ^{1}H NMR spectra and X-ray crystallographic studies. The Coordination mode of the synthesized ligand has been established by solid state isolation and physico-chemical identification of Co(III) and Cu(II) complexes, $[Co(HMHyP)_2]Cl$ (complex **II**), $[Co(HMHyP)_2]Br$ (complex **III**) and $[Cu(HMHyP)]NO_3$ (complex **IV**) respectively. All the reported coordination complexes are 1:1 electrolytic cationic species and the ligand behaves as a monodeprotonated 'NNO' tridentate one in all the complex species. IR spectral data indicate that the coordination of each of the metal centre of the complexes occurs through the pyrimidine nitrogen, azomethine nitrogen and hydroxyl oxygen atoms. X-ray crystallographic data have authenticated a CoN_4O_2 octahedral coordination for **II** and **III** (Triclinic (P-1) and Monoclinic ($P2_1/n$), respectively) and a CuN_2O_2 square planar coordination for **IV** (Triclinic (P-1)). All the synthesized compounds were tested for their DNA binding abilities and their mode of binding with DNA. Compounds **II, III & IV** show potential DNA binding activities with Salmon Testis DNA.

Keywords: Pyrimidine, Co(III), Cu(II), Crystal structures, Binding constant, Salmon Testis DNA

*Corresponding author. Fax: +91-33-25828282; e-mail: nitis.saha@gmail.com

1. Introduction

Bioinorganic chemistry is a fast developing field of modern chemistry that uses Schiff bases and their transition metal complexes for a variety of applications, e.g. in biological, medical, and environmental sciences [1]. The Schiff base ligands are quite popular because they are easily prepared by the condensation between carbonyl compounds and amines and also have some biochemical and analytical importance [2]. Hydroxy acetophenone can be used as primary compound for the synthesis of chalcones [3], flavones [4] etc. Schiff bases of Hydroxy aldehydes or, ketones are extensively used as coordinating ligands for the synthesis of metal complexes. Over the past decade, the syntheses of therapeutically active heterocyclic molecules have become one of the main areas of interest in synthetic chemistry [5]. These important structures have gained much consideration, because they are potentially active ligands and as well as of their binding capability towards various biological targets. Among these heterocycles, pyrimidines and their derivatives show various biochemical and agricultural applications [6]. Uracil (2,4-dihydroxypyrimidine) and thiamine (5-methyluracil) have immense importance in metabolism because these derivatives are basic units for RNA and DNA [7]. Pyrimidine ring systems in nucleic acids, vitamins and co-enzymes have some effective binding sites for metal ions. The presence of more than one hetero atom and the higher π acidity of the pyrimidine rings as compared to that of pyridine bases play an important role in coordination chemistry, and also serve as a better model in biological systems [8-10].

In the present communication, we have reported the syntheses, spectral and structural characterizations of a new NNO tridentate Schiff base ligand (H_2MH_yP) using 2-hydrazino-4,6-dimethylpyrimidine and substituted acetophenone and its Co(III) and Cu(II) complexes. The

details of DNA binding activities and mode of DNA binding of these complexes have also been reported.

2. Experimental

2.1 *Reagents and instrumentation*

All the reagents used were of AR grade and obtained from commercial sources and used without purification. Sodium salt of Salmon Testis DNA was purchased from Sigma-Aldrich. Spectrograde solvents were used for spectral measurements. Elemental analyses (C, H and N) were done with a Perkin-Elmer 2400 CHNS/O analyzer. The cobalt and copper contents of the complexes were determined gravimetrically as anhydrous $CoSO_4$ and iodometrically, respectively. Electronic spectra were recorded on a Shimadzu UV-2401PC spectrophotometer. IR spectra (4000–450 cm^{-1}) were recorded on a Perkin-Elmer L120-000A FT-IR spectrophotometer with KBr pellets. The molar conductance of the complexes in methanol were measured with a Systronics 304 digital conductivity meter. ^1H NMR spectrum of the ligand was recorded in DMSO-d_6 with a Bruker AC 400 superconducting FT NMR. High resolution mass spectroscopy (HRMS) was performed with a waters XEVO G2-S QTof mass spectrometer. A Rigaku FR-X Ultrahigh Brilliance Micro focus RA generator and Rigaku XtaLAB P200 system diffractometer was used to collect X-ray data of the complexes. Fluorescence measurements were done with a Perkin Elmer LS 55 Fluorescence spectrometer. Viscosity measurements were done with a Brookfield DV-II + Pro v6.3 Viscometer.

2.2 . Syntheses

*2.2.1. Synthesis of the ligand, H_2MH_yP (Compound **I**)*

2,4-dihydroxyacetophenone-4,6-dimethyhydrazino pyrimidine, H_2MH_yP [Fig. 1] was synthesized by refluxing an eqimolar mixture of 4,6-dimethyl-2-hydrazinopyrimidine [11-12] and 2,4-

dihydroxyacetophenone in dry ethanol involving conversion of dihydroxy acetophenone into its hydrazino pyrimidine derivative. A red crystalline solid was obtained after slow evaporation of the solvent. Crystals suitable for X-ray diffraction were obtained on slow evaporation of the compound **I** in ethanol. Yield of ca. 70–75% (m.p.: 182-183°C). *Anal.* Calcd for $C_{14}H_{16}N_4O_2$: C, 61.7; H, 5.9; N, 20.6. Found: C, 60.8; H, 5.5; N, 19.8%. IR (KBr) ν (cm^{-1}) : 1625 ($\nu_{CH=N}$), 3432 (ν_{C-OH}). ^{1}H NMR (DMSO-d_6) δ (ppm): 13.55 (1H, C_{10}-OH), 10.46 (1H, C_8-OH), 9.66 (1H, NH-hydrazine), 6.67 (1H, pyrimidine), 2.31(6H, 2-CH_3 pyrimidine), 2.26 (3H, C_5-CH_3). HRMS m/z: Calcd. for $C_{14}H_{17}N_4O_2$ $[M+H]^+$ 273.136, found 272.1358.

*2.2.2 Syntheses of complexes **II and III***

The reported Co(III) complexes have been prepared by refluxing ethanolic solution of the title ligand (**I)** (1.05mM) and $CoCl_2.6H_2O$ or $CoBr_2.6H_2O$ (0.525mM) in water bath for ~1 hr in presence of air. Dark brown coloured solution in both the cases, were obtained. On slow evaporation of the resulting solutions, the desired Co(III) complex, in each case, was separated out. The dark brown solids, in both the cases were filtered off, washed with cold ethanol and dried over anhydrous $CaCl_2$. Dark red crystals, in both the cases, were obtained from ethanol/ hexane mixture by slow diffusion, found suitable for X-ray crystallography. *Anal.* Calcd for $C_{28}H_{32}N_8O_5CoCl$ (**II**): C, 51.3; H, 4.9; N, 17.1; Co, 8.9. Found: C, 50.9; H, 4.3; N, 16.8; Co, 8.8%. IR (KBr) ν (cm^{-1}): 1637 ($\nu_{CH=N}$), 3515 (ν_{C-OH}). UV–Visible (DMSO, $\lambda_{max,}$ nm): 634 ($^1A_{1g} \rightarrow {}^3T_{2g}$), 375 ($^1A_{1g} \rightarrow {}^1T_{1g}$), 325($^1A_{1g} \rightarrow {}^1T_{2g}$), 265 (n→ π^*), 219 (π→ π^*). DRS ($\lambda_{max,}$ nm): 653 ($^1A_{1g} \rightarrow {}^3T_{2g}$), 412 ($^1A_{1g} \rightarrow {}^1T_{1g}$), 378 ($^1A_{1g} \rightarrow {}^1T_{2g}$). ^{1}H NMR (DMSO-$d_6$) δ (ppm): 13.06 (1H, OH), 9.654 (1H, NH- hydrazine), 2.506 (6H, 2-CH_3, pyrimidine), 2.27 (3H, C_5-CH_3). HRMS m/z: Calcd. for $C_{28}H_{30}N_8O_4Co$ $[M-Cl]^+$ 601.14, found 601.1713.

Anal. Calcd for $C_{30}H_{36}N_8O_5CoBr$ (**III**): C, 49.5; H, 4.9; N, 15.4; Co, 8.1. Found: C, 48.8; H, 4.5; N, 14.9; Co, 7.9%. IR (KBr) ν (cm^{-1}): 1639 ($\nu_{CH=N}$), 3497 (ν_{C-OH}). UV–Visible (DMSO, $\lambda_{max,}$ nm) : 633 ($^1A_{1g}\rightarrow{}^3T_{2g}$), 365 ($^1A_{1g} \rightarrow{}^1T_{1g}$), 310 ($^1A_{1g} \rightarrow{}^1T_{2g}$), 265 (n → π*), 220 (π→ π*). DRS ($\lambda_{max,}$ nm): 650 ($^1A_{1g}\rightarrow{}^3T_{2g}$), 410 ($^1A_{1g} \rightarrow{}^1T_{1g}$), 376 ($^1A_{1g} \rightarrow{}^1T_{2g}$). ^{1}H NMR (DMSO-$d_6$) δ (ppm): 13.0 (1H, OH), 9.52 (1H, NH-hydrazine), 2.504 (6H, 2-CH_3, pyrimidine), 2.23 (3H, C_5-CH_3). HRMS m/z: Calcd. for $C_{28}H_{30}N_8O_4Co$ $[M-Br]^+$ 601.19, found 601.1763.

*2.2.3 Synthesis of compound **IV***

The Cu(II) complex reported here, has been prepared by refluxing an equimolar (1.05mM) mixture of (**I**) and $Cu(NO_3)_2.3H_2O$ in ethanol for ~1hr. in a water bath. On slow evaporation of the resulting solution, reddish crystalline solids separated out, were filtered off, washed with cold ethanol and dried over anhydrous $CaCl_2$. Red brown crystals obtained from acetone/ hexane mixture were found to be suitable for X-ray diffraction. *Anal.* Calcd for $C_{14}H_{21}CuN_5O_8$: C, 37.3; H, 4.7; N, 15.5; Cu, 14.1. Found: C, 36.9; H, 4.3; N, 15.2; Cu, 13.8%. IR (KBr) ν (cm^{-1}): 1611 ($\nu_{CH=N}$). UV–Visible (DMSO, $\lambda_{max,}$ nm): 650 ($^2B_{1g} \rightarrow{}^2A_{1g}$). DRS ($\lambda_{max.}$ nm): 600 [$B_2(xy) \rightarrow A_1(x^2-y^2)$]. HRMS m/z: Calcd. for $C_{14}H_{15}N_4O_2Cu$ $[M-(NO_3+H_2O)]^+$ =334.66, found 334.0493.

2.3 Single crystal X-ray diffraction study

Data for compounds **I** to **IV** were collected on a Rigaku FR-X Ultrahigh Brilliance Micro focus RA generator /confocal optics and Rigaku XtaLAB P200 system with Mo-Kα radiation (λ = 0.71073 Å). Intensity data were collected using ω steps accumulating area detector images spanning at least a hemisphere of reciprocal space. All data were corrected for Lorentz polarization effects. A multi-scan absorption correction was applied using Crystal Clear [13]. Structures were

solved by direct methods (*SIR 2004* [14] or *SIR 2011* [15]) and refined by full-matrix least-squares against F^2 (*SHELXL-2013* [16]). All hydrogen atoms were assigned riding isotropic displacement parameters and constrained to idealize geometries, except those bound to N or O, which were located from the difference Fourier map and refined subject to a distance restraint. Hydrogen atoms could not be located for one of the water solvent molecules in **IV**. Neutral atom scattering factors were taken from International Tables for Crystallography (IT), Vol. C, Table 6.1.1.4 [17]. Anomalous dispersion effects were included in F_{calc} [18]. All calculations were performed using the Crystal Structure [19] interface, and figures were drawn using *OLEX2* [20].

2.4 DNA binding study

2.4.1. UV-Visible spectroscopic Study

The spectrophotometric studies were performed at 30^{o}C in Shimadzu (UV-2401PC) spectrophotometer using 1 cm path length rectangular quartz cuvette. To monitor the changes in absorption spectrum of DNA due to addition of complex II, III and IV, all of them was added gradually in each of the sample (containing DNA) and reference cuvettes. The absorbance of each complex (due to scattering) was systematically neglected by the addition of the same amount of complex in both suspensions of the cuvettes. Thereby, contribution due to scattering of compounds in DNA spectra was automatically nullified.

The interaction of the complex with the DNA was analyzed by the famous Hill equation [21]

This is stated below, $\text{Log } (Z / (1-Z)) = Y \text{ Log } K_b + Y \text{ Log } [C_f]$----------[1],

Where, $Z=(A_0-A_i)/(A_0-A_f)$ where, where A_0 is the (absorbance) 260 nm of DNA in the absence of complex, A_i the (absorbance) 260 nm of DNA at any complex concentration, and A_f the (absorbance) 260 nm of DNA at complex concentration for which interaction met saturation. Cf

and Kb were the free complex concentration and binding constant respectively. Moreover, Y is the co-operativity of the interaction of complex with respect to the DNA. The value as well sign both were important for the determination of the binding nature of the interaction. From the slope, the Y could be calculated which, was further used to determine the Binding constant using intercept of the equation. The importance of Y was that it characterized nature of co-operativity, that is, Y <1 signified negative co-operative nature of binding, Y = 1 signified non-co-operative nature of binding, and Y > 1 signified positive co-operative nature of binding [21].

2.4.2. Spectrofluorimetric study

The fluorescence quenching measurements were done by using Perkin Elmer LS 55 Fluorescence spectrometer. Both the compounds as well as free DNA have no characteristic fluorescence. But intercalation of EB increased the fluorescence intensity which was used to observe the binding behavior of DNA with respect to the compounds. The said Salmon Testis DNA were prepared in sterile Tris buffer (50 mM, pH 7.5) of 1mg/ ml stock by mild sonication at 4^0C in presence of ice, so that the linear DNA was broken into uniform size. Further the DNA was incubated with saturating amount of EB (10 mg/ ml in sterile water) in dark for another 30 mins where, complete intercalation of EB took place. Now the EB–DNA was excited at 480 nm and the emission was monitored in between 500 to 700 nm with an emission maximum at around 600 nm. The emission slit width (10 nm) and scan rate (200 nm /min) were kept constant for all the measurements.

In order to demonstrate the measure of the threshold DNA concentration and the binding constants, the fluorescence data were further analyzed according to the simplified form of the Scatchard equation [22]:

$r/C_f = K_b(1-nr)$ ----------[2]

The Scatchard equation was plotted to measure the binding constant between bio-macromolecule and compounds. Where, $r = C_b/CDNA$, $C_b = C_t - C_f$. C_f, C_b and C_t are the compounds concentrations of free form, bound form and the total form respectively, K_b is the binding constant, n is the number of binding sites expressed by DNA base pairs.

2.4.3. Viscometric study

In order to understand the mode of DNA complex interaction – intercalation or groove binding – a viscometric study was carried out as the most authentic test [23]. Viscosity measurements were carried out with a micro viscometer (Model Brookfield DVII+pro-v6.3) attached to a water-bath at 30^{o}C. The viscosity of DNA in absence of any complex was first quantitated, followed by the measurements after addition of increasing concentration of compounds (II, III and IV) into the DNA up to its saturation separately. After each addition of complex, 1.5 min was allowed to attain thermal equilibrium and then the viscosity was measured individually. The viscometric data was calculated maintaining viscometric rotor stirring at 100 rpm and each measurement was repeated three times in order to find out the average of value. The data were plotted as $(\eta/\eta_0)1/3$ versus r, where η and η_0 signified the viscosity of DNA in the presence and absence of complex respectively and r represented the molar ratio of complex: DNA.

3. Result and Discussion

3.1. Crystal structures of H_2MHyP (I), [Co(HMHyP)$_2$]Cl (II), [Co(HMHyP)$_2$]Br (III) and [Cu(HMHyP)]NO_3 (IV)

The molar conductance values in MeOH (30^oC) indicate 1:1 electrolytic character of the complexes [24] and conform to the general compositions, *[Co(HMHyP)$_2$]Cl* (X= Cl and Br) and *[Cu(HMHyP)]NO$_3$*.

Views of the X-ray structures of the free ligand (H_2MHyP) (**I**), and its metal complexes- [Co(HMHyP)$_2$]Cl (**II**), [Co(HMHyP)$_2$]Br (**III**) and [Cu(HMHyP)]NO_3 (**IV**) with atom numbering scheme are shown in Figs 2, 3, 4 and 5, respectively. The crystallographic data and refinement parameters are summarized in Table **1**. The structure of the primary ligand molecule **I** has an asymmetric unit comprising an H_2MHyP molecule and a molecule of water of crystallization. The structures of complexes **II** to **IV** have asymmetric units comprising a molecule of mononuclear metal complex, anion and solvent of crystallization. Some selected bond distances and bond angles of four structures are compiled and compared in Table **2**. The structure of ligand (**I**) (Fig. 2) shows that the neutral ONN tridentate ligand has a planar arrangement, with O1 and N4 positioned to interact via an O–H···N hydrogen bond, and with the N3–N4 bond oriented to minimize steric interactions between the pyrimidyl and N-methyl groups. The structures of compounds **II** and **III** show that they adopt related distorted octahedral geometries, (Figs 3 & 4, respectively). In both cases the Co(III) centers are coordinated in a N_4O_2 fashion by two mono-deprotonated ligands, using pairs of cis pyrimidyl-N, trans-azomethine-N and cis- hydroxyl-O atoms. The two pyrimidyl nitrogen atoms (N1 and N5) and two hydroxyl oxygen atoms (O1 and O3) are located in the square plane, with the two azomethine nitrogen atoms (N4 and N8) occupying the axial positions, both ligands binding in meridional fashion, and retaining a degree of planarity. One of the two ligands in complex **II** appears to be showing a tautomeric form. Its C1–N2 bond distance [1.372(3) Å] is longer than those observed for free ligand [1.3427(14) Å]; additionally, the C1-N3 bond [1.302(3) Å] is correspondingly shorter than the equivalent bond in the free ligand [1.3675(15) Å]. These

changes in bond distances, combined with the inability to locate a hydrogen atom on N3 of one ligand, instead finding it at N2, is indicative of the presence of double bond character for the C1-N3 bond, and single bond character for the C1-N2 bond. No such significant bond shortening is observed in either the second ligand of complex **II** or in complexes **III** and **IV**. The structure of compound **IV** (Fig. 5) shows it adopting a distorted square-planar geometry. The Cu(II) centre is coordinated in an N_2O_2 fashion by a mono-deprotonated ligand, using pyrimidyl-N, azomethine-N, hydroxyl-O, as well as a coordinated water molecule. The deviation of Cu^{2+} from the square plane is 0.0162(13) Å.

Table **3** gives the details of the hydrogen bonding interactions of the four reported compounds. Each molecule of compound **I** is connected via two O–H···O hydrogen bonds to adjacent water molecules, forming one-dimensional zigzag chains running along the crystallographic *c*-axis. These chains are connected into 2D sheets in the ac plane by further O–H···N hydrogen bonds between the water and one pyrimidine nitrogen (Fig. 6). In compound **II**, each molecule of the complex is connected via two O–H···Cl and one $N_{pyrimidyl}$–H···Cl hydrogen bonds to three adjacent chloride anions, and via one $N_{hydrazinyl}$–H···O hydrogen bond to the adjacent water molecule. Each chloride in turn is a total of four hydrogen-bonding interactions, two hydroxyl-OH, one pyrimidyl-NH and one water-OH, while the water molecule acts as donor for two hydrogen bonds, one to chloride, the other to one hydroxyl-O. This arrangement of interactions results in the formation of a topologically complex three-dimensional hydrogen-bonded network (Fig. 7). In contrast to compound **II**, showing no hydrogen bonds between adjacent complexes, compound **III** forms one-dimensional hydrogen-bonded chains propagating along the *a*-axis via O–H···O interactions between O2 and O4. These chains are linked into two-dimensional sheets in the *ac* plane by two O–H···Br (one from the complex, the other from EtOH), one N–H···Br and one N–H···O

hydrogens bonds (Fig. 8). In compound **IV** each complex is connected to an adjacent complex by O-H···O hydrogen bonds between the coordinated water and two bridging nitrate anions, forming a dinuclear hydrogen-bonded complex. These complexes are linked together by N–H···O hydrogen bonds to form a double-layer zigzag chain running along the *ab*-diagonal axis. The two water molecules are found to hydrogen bond at the periphery of this chain. Due to the inability to locate hydrogen atoms on one water it is difficult to determine what forth hydrogen-bonding interactions would arise from it, however its positioning suggests that the two water molecules could be involved in interactions linking adjacent (Fig. 9).

3.2. DNA Interaction Studies

3.2.1. Stability of the complexes in solution

The solution spectrum (in DMSO) of each reported complex species is similar in nature with the spectrum obtained in solid state (DRS), indicating no gross electronic or geometric change occurs on dissolution of the complex in the solvent; the HRMS studies of all the compounds in methanol showed satisfactory result in each case (data included in the text). Moreover, the stability of the complex species in solution has been studied by taking UV-Vis spectra of each complex species immediately after dissolution in the said solvent (zero hr) and after 48 hrs of incubation at RT. It has been observed that in each case the spectral nature is grossly similar (Figs. S1-S3), indicating the retention of structure in solution.

3.2.2. UV-Visible spectroscopic study

The absorbance at 260 nm of ST DNA in the presence of 50 mM Tris Buffer decreased gradually with the increment of the each complex concentration and there was a sign of interaction between compounds with respect to DNA Fig.10(a)-(c). The binding isotherm of DNA–complex

interaction (not shown) represented sigmoidal nature of interaction indicating cooperative nature of DNA complex bindings. Form the derived log plot by Figs 12(a), 13(a) and 14(a), both the binding constant as well as Y could be calculated. The binding constant (K) for each case has been calculated and found to be 16.9 x 10^3 M^{-1}, 19.9 x 10^3 M^{-1} and 16.4 x 10^3 M^{-1} for the compounds **II**, **III** and **IV**, respectively. The Y value of the also was determined from the slope of the straight line which was found to be 4.4, 3.1 and 3 respectively for the compounds **II**, **III** and **IV**. The positive sign of the Y indicated that the interaction was highly co-operative.

*3.2.1. Fluorescence quenching of EB–DNA by compound **II**, **III** & **IV***

Ethidium bromide (EB) can be used as the fluorescence probe for DNA to study the molecular interactions between DNA and the compounds in the excited state. Though EB is a moderate fluorophore, but in presence of DNA it provides powerful fluorescence maximum at 600 nm on excitation at 480nm due its strong binding power with two nucleotide base pairs in intercalated state. The enhanced fluorescence of EB-DNA can be reduced by the addition of another interacting molecule [25, 26]. In the present systems, we have studied the effects of pyrimidine containing Schiff base ligand (**I**) and its metal compounds (**II**, **III** and **IV**) on the DNA through fluorescence emission spectral studies. Compound **I** didn't show any fluorescence emission on interaction with EB-DNA. [Fig. 11(a)-(c)]. It has been observed that the addition of compounds **II**- **IV** (suspended in DMSO solution**)** to a solution of EB bound DNA resulted in a decrease in fluorescence emission intensity in each case, which may be due to the quenching of fluorescence takes place upon interaction between DNA and metal compounds. The fluorescence quenching is quantitated by the Stern–Volmer relation:

$$\mathbf{F_0/F = 1 + K_{sv}[Q]} \quad \text{……...[3]}$$

Where, F_0 and F are the emission intensities of the fluorophore in absence and in presence of quencher, respectively. K_{sv} is the stern-volmer (SV) constant [27]. [Q] is the concentration of the interacting molecule i.e.; quencher. According to equation (1), we obtained a linear plot for F_0/F against each quencher [Figs. 12(b), 13(b) and 14(b)]. From the slopes of the straight line, we have calculated the SV constants for the quenchers (K_{SV} = 2.9 x 10^3 for **II**, 3 x 10^3 for **III** and 1 x 10^3 M^{-1} for **IV**).

Moreover the relation of K_{sv} with K_q is $K_{sv}=K_q$ X Γ where, K_q and Γ were quenching constant and the lifetime of flour, respectively [28]. The value of K_q determined the nature of quenching, as the higher value than the limiting value (limiting value of 1 X 10^{10} $M^{-1}s^{-1}$) denoted the static quenching whereas, the lower value denoted the dynamic ones. It was reported that the Γ value for DNA-EB was in the range of 23 ns [27]. Thus the observed K_q found to be 12.6 X 10^{10} $M^{-1}s^{-1}$, 13.04 X 10^{10} $M^{-1}s^{-1}$ and 4.31 X 10^{10} $M^{-1}s^{-1}$ for the compounds **II**, **III** and **IV**, respectively. The obtained bimolecular quenching constant (kq) was much larger than the limiting value of 1 X 10^{10} $M^{-1}s^{-1}$, which was considered the maximum positive value in fluorescence quenching in aqueous conditions. Thus dynamic quenching may be cancelled for the quenching of EB–DNA fluorescence by each of the compound.

The binding constant (K) for each case has been calculated according to the Scatchard equation as mention above and found to be 13.2 X 10^3 M^{-1}, 19.9 X 10^3 M^{-1} and 12.8 X 10^3 M^{-1} for the compounds **II**, **III** and **IV**, respectively [Figs 12(c), 13(c) and 14(c),]. The numbers of binding sites (n) are obtained as 2.15, 1.56 and 3.57 for **II**, **III** and **IV**, respectively. The values of ‘‘n” was found to be in the range of 2-4 and existence of multiple binding sites in DNA for all the compounds. The more than one binding sites was also supported nature of co-operative interactions at ground states observed in UV-Visible study. That In general the pyrimidine ring

structure somehow replaced the EB and might be intercalated between base pairs, thereby, repelling the EB from the said position causing decrease in fluorescence intensity. The binding constant of these two types of compounds (both octahedral Co(III) and square planner Cu(II)) are of the same order**.** Actually DNA ligand interaction solely depend not only the architecture of the DNA but also of ligand structure. As both ligands of these two compounds remained same thereby there are some common strategies to replace the bound EB from the DNA or quenching the fluorescence of the DNA-EB compounds by metal upon complexation. The latter is true as EB-DNA interaction are stronger than the DNA ligand interactions (almost comparable), thus the quenching process are carried out by metal compounds (the contribution of the free ligand DNA interaction is minimum (data not shown). Thus the both compounds would have almost same range of binding strength.

3.2.3. Viscometric study

Hydrodynamic method, such as changes in viscosity, which is exquisitely dependent to the change of length of DNA, may be the most effective means studying the binding mode of compounds to DNA. To confirm the interaction mode of the complex with DNA, a viscosity study was performed. Groove-binding typically resulted in only a few changes in structure in the backbone keeping the DNA essentially in an unaltered in naturally B-form, whereas intercalation resulted in an increase in the length DNA structure due to insertion of planar ligand moiety between adjacent base pairs [23, 29]. Thus intercalation of compound inside the DNA base pairs caused lengthening, stiffening and unwinding of the helix resulting with a pronounced increment of the intrinsic viscosity. Thus increase in viscosity signified intercalation mode of interaction rather than groove binding ones. Our preliminary study showed that gradual increase of viscosity with the rise of

compound concentrations [Figs 12(d), 13(d) and 14(d)]. This increase in viscosity proved that all of the metal compounds intercalated inside the DNA base pairs.

4. Conclusion

The present communication provides a general and effective method for the synthesis of 2,4-dihydroxyacetophenone-4,6-dimethylhydrazino pyrimidine, H_2MH_yP and its Co(III) and Cu(II) complexes. All the compounds are monomeric in nature and crystallize in either monoclinic (**I** & **III**) or triclinic (**II** & **IV**) crystal system; with nearly octahedral and square planar geometries for Co(III) and Cu(II) complexes, respectively. Compounds **II**, **III** & **IV** show potential DNA binding activities with Salmon Testis DNA due to their positive metal Centre's. The order of association constant all of the compounds are in the range of 10^4 M^{-1} at both ground and excited states which is quite high. The nature of quenching is static with an intercalation mode of bindings in all the synthesized compounds.

Acknowledgments

One of us (Rajesh Pradhan) is thankful to the University of Kalyani for providing financial support in the form of University Research fellowship. The financial support received from the DST-PURSE program and the UGC-SAP DRS-II program, University of Kalyani, is thankfully acknowledged. We are thankful to Professor Nilmoni Sarkar, Department of Chemistry, Indian Institute of Technology, Kharagpur, for providing us viscometric facility.

Appendix A. Supplementary material

Crystallographic data for the structures reported here have been deposited with the Cambridge Crystallographic Data Center, CCDC Nos 1015148, 1015149, 1015150 and 1015151. Copies of this information may be obtained free of charge from the Director, CCDC, 12 Union Road, Cambridge, CB2 1EZ, UK (Fax: +44-1223-336-033); E-mail: deposit@ccdc.cam.ac.uk or http://www.ccdc.cam.ac.uk. Figures S1-S3 are available as supplementary materials.

References

[1] P. Sathyadevi, P. Krishnamoorthy, R.R. Butorac, A.H. Cowley, N. Dharmaraj, Metallomics 4 (2012) 498.

[2] N.E.A. El-Gamel, RSC Advan. 2 (2012) 5870.

[3] Y.S. Nalwar, M.A. Sayyed, S.S. Mokle, P.R. Zanwar, Y.B. Vibhute, W.J. Chem. 4 (2009) 123.

[4] S.S. Mokle, M.A. Sayyed, K. Chopde, Int. J. Chem. Sci. 2 (2004) 96.

[5] S. Nahid, G. Zeinab, H. Saba, Bioinor. Chem. and Appl. 2012 (2012) (Article ID 126451)

[6] J. Hung, L.M. Werbel, J. Heterocycl. Chem. 21 (1984) 741.

[7] R.M. Abdel-Rahman, A.M. Abdel-Halim, Commun. Fac. Scien. Univ., Ankara, *B*31 (1985).

[8] F. Zamora, M. Kunsman, M. Sabat, B. Lippart, Inorg. Chem. 36 (1997) 1583.

[9] M. Louloudi, Y. Deligiannakis, J.P. Tuchagues, B. D, N. Hadjiliadis. Inorg. Chem. 36 (1997) 6335.

[10] F. Jolibois, J. Cadet, A. Grand, R. Subra, N. Rega, V. Barone. J. Am. Chem. Soc. 120 (1998) 1864.

[11] G.M. Kosolapoff, C.H. Roy, J. Org. Chem. 26 (1961) 1895.

[12] M.P.V. Boarland, J.F.W. McOmie, R. N. Timms, J. Chem. Soc. (1952) 4691.

[13] Crystal Clear-SM Expert v2.1. Rigaku Americas, the Woodlands, Texas, USA, and Rigaku Corporation, Tokyo, Japan, 2010-2014.

[14] M.C. Burla, R. Caliandro, M. Camalli, B. Carrozzini, G.L. Cascarano, L.D. Caro, C. Giacovazzo, G. Polidori, R. Spagna, J. Appl. Cryst. 38, (2005) 381.

[15] M.C. Burla, R. Caliandro, M. Camalli, B. Carrozzini, G.L. Cascarano, C. Giacovazzo, M. Mallamo, A. Mazzone, G. Polidori, R. Spagna, J. Appl. Cryst. 45 (2012) 357.

[16] G.M. Sheldrick, Acta Crystallogr., Sect. A 64 (2008) 112.

[17] International Tables for Crystallography, Vol.C Ed. A.J.C. Wilson, Kluwer Academic Publishers, Dordrecht, Netherlands, Table 6.1.1.4, pp. (1992) 572.

[18] J.A. Ibers, W.C. Hamilton, Acta Crystallogr. 17 (1964) 781.

[19] Crystal Structure v4.1. Rigaku Americas, the Woodlands, Texas, USA, and Rigaku Corporation, Tokyo, Japan, (2013).

[20] O.V. Dolomanov, L.J. Bourhis, R.J. Gildea, J.A.K. Howard, H. Puschmann, J. Appl. Cryst. 42 (2009) 339.

[21] M. Banik, T. Basu, Dalton Trans, 43 (2014) 3244.

[22] G. M. Howe, K. C. Wu, W. R. Bauer, Biochem. 15 (1976) 4339.

[23] S. Tabassum, A. Asim, F. Arjmand, Md. Afzal, V. Bagchi, Eur. J. Med. Chem., 58 (2012) 308.

[24] W.J. Geary, Coord. Chem. Rev., 7 (1971) 81.

[25] B.C. Baguley, M. LeBret, Biochem., 23 (1984) 937.

[26] J.R. Lakowicz, G. Webber, Biochem., 12 (1973) 4171.

[27] A. Kathiravan, R. Renganathan, Polyhedron 28 (2009) 1374.

[28] J.R. Lakowicz, Princ. Fluores. Spectros. , Springer, New York, (2006).

[29] S. Roy, S. Saha, R. Majumdar, R. R. Dighe, A. R. Chakravarty, Polyhedron, 29 (2010) 2787.

Figure captions

Figure 1. Structural Formulation of the ligand (H_2MHyP).

Figure 2. View of the asymmetric unit (crystallographic numbering) of **I**. Thermal ellipsoids are drawn at the 50 % probability level.

Figure 3. View of the asymmetric unit (crystallographic numbering) of **II**. Thermal ellipsoids are drawn at the 50 % probability level.

Figure 4. View of the asymmetric unit (crystallographic numbering) of **III**. Thermal ellipsoids are drawn at the 50 % probability level.

Figure 5. View of the asymmetric unit (crystallographic numbering) of **IV**. Thermal ellipsoids are drawn at the 50 % probability level.

Figure 6. Views of the two-dimensional hydrogen-bonded sheet formed by **I**. Hydrogen atoms not involved in hydrogen bonding are omitted. (top) View down the b-axis of the sheet in the ac-plane. (Bottom) View down the a-axis of two adjacent corrugated sheets.

Figure 7. View down the c-axis of the three-dimensional hydrogen-bonded network formed by **II**. Hydrogen atoms not involved in hydrogen bonding are omitted.

Figure 8. Views of the two-dimensional hydrogen-bonded sheet formed by **III**. Hydrogen atoms not involved in hydrogen bonding are omitted. (top) View down the b-axis of the sheet in the ac-plane. (bottom) View down the a-axis of corrugated sheet.

Figure 9. View down the ac-diagonal axis of the one-dimensional hydrogen bonded double-layered chains formed by **IV**, running along the ab-diagonal axis Hydrogen atoms not involved in hydrogen bonding are omitted.

Figure 10. UV-Vis. Absorption titration of Salmon Testis-DNA in the presence of various concentrations
(a) compound **II** ([comp. **II**] = 0-160 μM)**;**
(b) compound **III** ([comp. **III**] = 0-125 μM**);**
(c) compound **IV** ([comp. **IV**] = 0-160 μM).

Figure 11. Fluorescence quenching of EB–DNA in the presence of various concentrations **(a)** compound **II**(λ_{max}= 480 nm; λ_{emi}= 600 nm; [comp. **II**] = 0-600 µM**);** **(b)** compound **III**(λ_{max}= 480 nm; λ_{emi}= 600 nm; [comp. **III**] = 0-600 µM**);** **(c)** compound **IV**(λ_{max}= 480 nm; λ_{emi}= 600 nm; [comp. **IV**] = 0-1050 µM).

Figure 12. (a) Hill plot of compound **II** (**[**comp. **II**]**=** 0-160 µM) with DNA interaction; **(b)** Stern-Volmer plot of DNA-EtBr with compound **II** (λ_{max}= 480 nm; λ_{emi}= 600 nm; [comp. **II**] = 0-530 µM); **(c)** Derived Scatchard plot of compound **II** in the excited state range; **(d)** Viscometric study of compound **II** with DNA (keeping DNA conc. 300 µM with a gradual addition of varying conc. of compound **II** with a maximum ratio of 0.5).

Figure 13. **(a)** Hill plot of compound **III** (**[**comp. **III**]**=** 0-125 µM) with DNA interaction; **(b)** Stern-Volmer plot of DNA-EtBr with compound **III** (λ_{max}= 480 nm; λ_{emi}= 600 nm; [comp. **III**] = 0-600 µM); **(c)** Derived Scatchard plot of compound **III** in the excited state range; **(d)** Viscometric study of compound **III** with DNA (keeping DNA conc. 300 µM with a gradual addition of varying conc. of compd. **III** with a maximum ratio of 0.7).

Figure 14. **(a)** Hill plot of compound **IV** (**[**comp. **IV**]**=** 0-160 µM) with DNA interaction; **(b)** Stern-Volmer plot of DNA-EtBr with compound **IV** (λ_{max}= 480 nm; λ_{emi}= 600 nm; [comp. **IV**] = 0-1050 µM); **(c)** Derived Scatchard plot of compound **III** in the excited state range; **(d)** Viscometric study of compound **IV** with DNA (keeping DNA conc. 300 µM with a gradual addition of varying conc. of compd. **IV** with a maximum ratio of 1.3).

Figure S1. (a) Solid state UV-Vis spectra (DRS) of compound **II**; **(b)** UV-Vis spectra of compound **II** (200-400nm) in DMSO; **(c)** UV-Vis spectra of compound **II** (400-900nm) in DMSO.

Figure S2. **(a)** Solid state UV-Vis. spectra (DRS) of compound **III; (b)** UV-Vis spectra of compound **III** (200-400nm) in DMSO; **(c)** UV-Vis spectra of Compound **III** (400-900nm) in DMSO.

Figure S3. **(a)** Solid state UV-Vis. spectra (DRS) of compound **IV**; **(b)** UV-Vis spectra of compound **IV** (200-400nm) in DMSO; **(c)** UV-Vis spectra of compound **IV** (400-900nm) in DMSO.

Table 1. Crystal data and structure refinement parameters for $C_{14}H_{18}N_4O_3$ (I), $C_{28}H_{32}ClCoN_8O_5$ (II), $C_{30}H_{36}BrCoN_8O_5$ (III), and $C_{14}H_{21}CuN_5O_8$ (IV)

Crystal data	I	II	III	IV
Empirical Formula	$C_{14}H_{18}N_4O_3$	$C_{28}H_{32}ClCoN_8O_5$	$C_{30}H_{36}BrCoN_8O_5$	$C_{14}H_{21}CuN_5O_8$
Formula Weight	290.32	655.00	727.50	450.89
Crystal System	Monoclinic	Triclinic	Monoclinic	Triclinic
Space Group	$P2_1/c$ (#14)	P-1 (#2)	$P2_1/n$ (#14)	P-1 (#2)
Temperature (K)	173	173	173	173
Wavelength (Å)	0.71075	0.71075	0.71075	0.71075
a [Å]	8.8142(10)	9.9443(15))	11.4355(9)	6.9710(9)
b [Å]	11.5377(14)	12.5537(18)	15.3368(14)	9.7780(12)
c [Å]	14.2644(17)	12.617(2)	18.3422(18)	13.8111(18)
α [°]	90	105.014(3	90	99.403(3)
β [°]	91.215(4)	91.543(3)	104.116(3)	99.091(2)
γ [°]	90	105.753(3)	90	101.985(3)
Volume [$Å^3$]	1450.3(3)	1456.1(4)	3119.8(5)	890.4(2)
Z, $D_{calc.}$ [gm/cm^3]	4, 1.330	2, 1.494	4, 1.549	2, 1.682
F (000)	616	680	1496	466
Crystal size [mm]	0.27X 0.10 X 0.06	0.10X 0.03 X 0.02	0.22 X 0.10 X 0.06	0.11X0.07 X0.02
θ ranges (°)	2.27 to 25.37	1.68 to 25.43	1.75 to 25.42	1.53 to 25.42
Limiting indices	-10 <= h <= 10	-12 <= h <= 12	-13 <= h <= 13	-8 <= h <= 8
	-13 <= k <= 13	-15 <= k <= 15	-18 <= k <= 18	-11 <= k <= 11
	-17 <= l <= 16	-15<= l <= 15	-22 <= l <= 22	- 16 <= l <= 16
Reflections collected	17364	17997	37604	11039
Unique reflections	2663 [R(int) = 0.0400]	5321 [R(int) = 0.0507]	5737 [R(int) = 0.0305]	3246[R(int)=0.0429]
Refinement method	Full-matrix least	Full-matrix least	Full-matrix least	Full-matrix least
	-Squares on F^2	-Squares on F^2	-Squares on F^2	-Squares on F^2
Data / parameters	2663/ 208	5321/ 418	5737/ 433	3246 / 276
Goodness-of-fit on F^2	1.086	0.977	1.061	1.064
Final R indices [I>2σ (I)]	R1= 0.0383	R1= 0.0312	R1 = 0.0286	R1= 0.0550
R indices (all data)	R1 =0.0427	R1 =0.0360	R1 = 0.0314	R1 =0.0594
	*w*R2 =0.1164	*w*R2 =0.0837	*w*R2 = 0.0824	*w*R2 =0.1474
Min. and Max. Resd. Dens.[e/ $Å^3$]	-0.20 and 0.24	-0.33 and 0.40	-0.38 and 0.90	-1.44 and 1.59

Table 2. Selected bond lengths (Å), bond angles and torsion angles (°) of $C_{14}H_{18}N_4O_3$ (I), $C_{28}H_{32}ClCoN_8O_5$ (II), $C_{30}H_{36}BrCoN_8O_5$ (III) and $C_{14}H_{21}CuN_5O_8$ (IV)

	I	II	III	IV
Bond lengths				
N1–C1	1.3393(14)	1.384(2)	1.353(3)	1.347(5)
N5-C15	-	1.357(2)	1.355(3)	-
N2-C1	1.3427(14)	1.372(3)	1.329(3)	1.339(5)
N6-C15	-	1.332(2)	1.327(3)	-
N1–C2	1.3379(15)	1.335(3)	1.363(3)	1.368(6)
N5-C16	-	1.357(3)	1.360(2)	-
N3–C1	1.3675(15)	1.302(3)	1.369(2)	1.365(6)
N7–C15	-	1.352(3)	1.363(2)	-
N3–N4	1.3631(14)	1.396(2)	1.391(3)	1.383(4)
N7–N8	-	1.3901(19)	1.398(3)	-
N4–C5	1.2895(15)	1.307(2)	1.305(2)	1.306(6)
N8–C19	-	1.299(3)	1.299(2)	-
O1–C8	1.3646(14)	1.326(2)	1.323(2)	1.314(6)
O3–C22	-	1.316(2)	1.315(2)	-
M1–N1	-	1.9791(19)	1.9869(18)	2.010(3)
M1–N5	-	2.0007(15)	1.9701(18)	-
M1–N4	-	1.8791(14)	1.8978(17)	1.932(4)
M1–N8	-	1.8893(14)	1.8968(17)	-
M1–O1	-	1.8476(15)	1.8656(15)	1.873(3)
M1–O3	-	1.8574(12)	1.8755(14)	-
M1–O3(W)	-	-	-	1.975(3)
Bond angles				
C1-N1-C2	115.62(10)	117.98(18)	116.08(18)	115.7(3)
N4-N3-C1	118.05(9)	109.46(15)	114.83(17)	116.8(3)
N3-N4-C5	122.46(9)	116.71(15)	118.12(17)	117.7(3)
N1-C1-N2	127.16(10)	119.30(18)	127.28(18)	127.6(4)
N2-C1-N3	115.12(9)	118.08(17)	115.22(19)	114.6(4)
N1-C1-N3	117.72(10)	122.62(18)	117.45(19)	117.7(3)
N4-C5-C7	114.83(9)	119.55(16)	119.10(19)	120.1(4)
C5–C7–C8	122.07(10)	122.64(16)	121.17(17)	124.0(4)
O1-C8-C7	122.40(10)	124.37(19)	123.6(2)	124.5(3)
C7-C8-C9	120.95(10)	119.68(17)	119.45(17)	118.7(4)
N1-M1-N4	-	81.45(7)	83.09(7)	83.17(14)
N5-M1-N8	-	81.52(6)	83.26(7)	-
O1-M1-N4	-	92.86(7)	90.59(7)	92.39(13)
O3-M1-N8	-	91.45(6)	92.31(7)	-
N1-M1-N8	-	97.13(7)	102.76(7)	-
N1-M1-N5	-	86.51(7)	96.70(7)	-
N4-M1-N5	-	96.91(6)	99.13(7)	-
N4-M1-N8	-	177.97(6)	173.44(7)	-
O1-M1-N8	-	88.47(7)	83.40(7)	-
O3-M1-N4	-	90.03(6)	84.95(6)	175.18(14)
O1-M1-N1	-	173.64(7)	172.95(7)	173.13(14)
O1-M1-N5	-	91.37(7)	87.36(7)	-
O3-M1-N1	-	91.00(6)	87.25(7)	-
O3-M1-N5	-	172.19(6)	174.62(7)	-
O1-M1-O3	-	91.86(6)	89.08(6)	-

Table 3. Hydrogen bonding distances (Å) and angles (◦)

D-H···A	D-A(Å)	D-H(Å)	H···A(Å)	<D-H···A(◦)	symmetry
		Compound 1			
O1-H1···N1 (intramol)	3.3406(13)	0.965(16)	2.567(17)	137.3(15)	-
O1-H1···N4 (intramol.)	2.5226(12)	0.965(16)	1.645(16)	149.0(17)	-
O2-H2··· O21	2.6814(14)	0.934(17)	1.764(17)	166.7(17)	X+1, Y+1/2, Z+1/2-1
O21-H21A···O1	2.7855(12)	0.930(15)	1.873(15)	166.6(15)	X-1, Y, Z
O21-H21B···N2	2.7840(13)	0.944(16)	1.961(17)	144.5(14)	-
N3-H3···O21	2.9859(14)	0.912(13)	2.222(13)	140.9(12)	-
		Compound II			
O2-H2···Cl1	3.0229(15)	0.904(17)	2.121(18)	176(3)	X, Y, Z+1
O4-H4···Cl1	3.0350(16)	0.929(16)	2.120(17)	168(2)	-X+1,-Y+1,-Z+1
O31- H31A··· Cl1	3.190(2)	0.940(17)	2.273(18)	165(2)	-
O31-H31B··· O2	2.905(2)	0.951(18)	1.98(2)	163(3)	-X+1,-Y,-Z+1
N2-H2A···Cl1	3.159(2)	0.948(17)	2.267(19)	156(2)	-
N7-H7···O31	2.805(2)	0.923(16)	1.897(17)	167(2)	X-1, Y, Z
		Compound III			
O2-H2···O4	2.756(3)	0.934(17)	1.831(18)	171(3)	X-1, Y, Z
O4-H4···Br1	3.1614(16)	0.936(18)	2.24(2)	167(3)	-X+2, -Y, -Z+2
O31-H31···Br1	3.241(2)	0.945(17)	2.340(19)	159(2)	-X+1/2+1, Y+1/2, -Z+1/2+1
N3-H3···O31	2.760(3)	0.932(17)	1.864(18)	160(2)	-
N7-H7···Br1	3.4703(18)	0.952(17)	2.57(2)	158(2)	-X+1, -Y, -Z+2
		Compound IV			
O2-H2···O31	2.685(7)	0.96(2)	1.74(2)	170(6)	X, Y-1, Z
O3-H3B···O21	3.191(11)	0.96(2)	2.37(4)	143(5)	X, Y-1, Z
O3-H3B···O23	2.998(8)	0.96(2)	2.07(3)	163(5)	X, Y-1, Z
O3-H3C···O21	2.725(5)	0.96(2)	1.84(3)	153(6)	-X+1, -Y, -Z+1
O31-H31A···O23	3.004(10)	0.97(2)	2.03(3)	173(11)	-X+1, -Y+1, -Z+1
O31- H31B···O41	3.36(3)	0.98(2)	2.51(8)	144(10)	-X, -Y+1, -Z+1
N3-H3A···O22	2.965(6)	0.96(2)	2.07(3)	156(4)	X+1, Y, Z

Figure 1

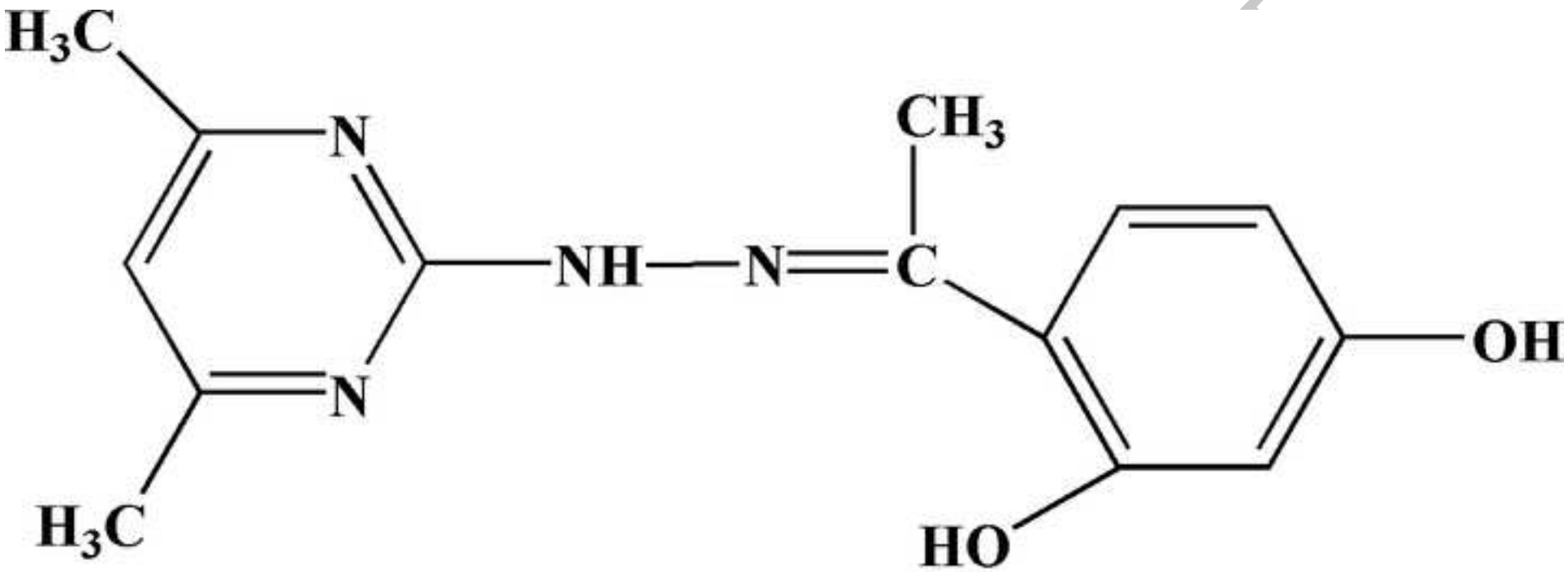

Figure 2

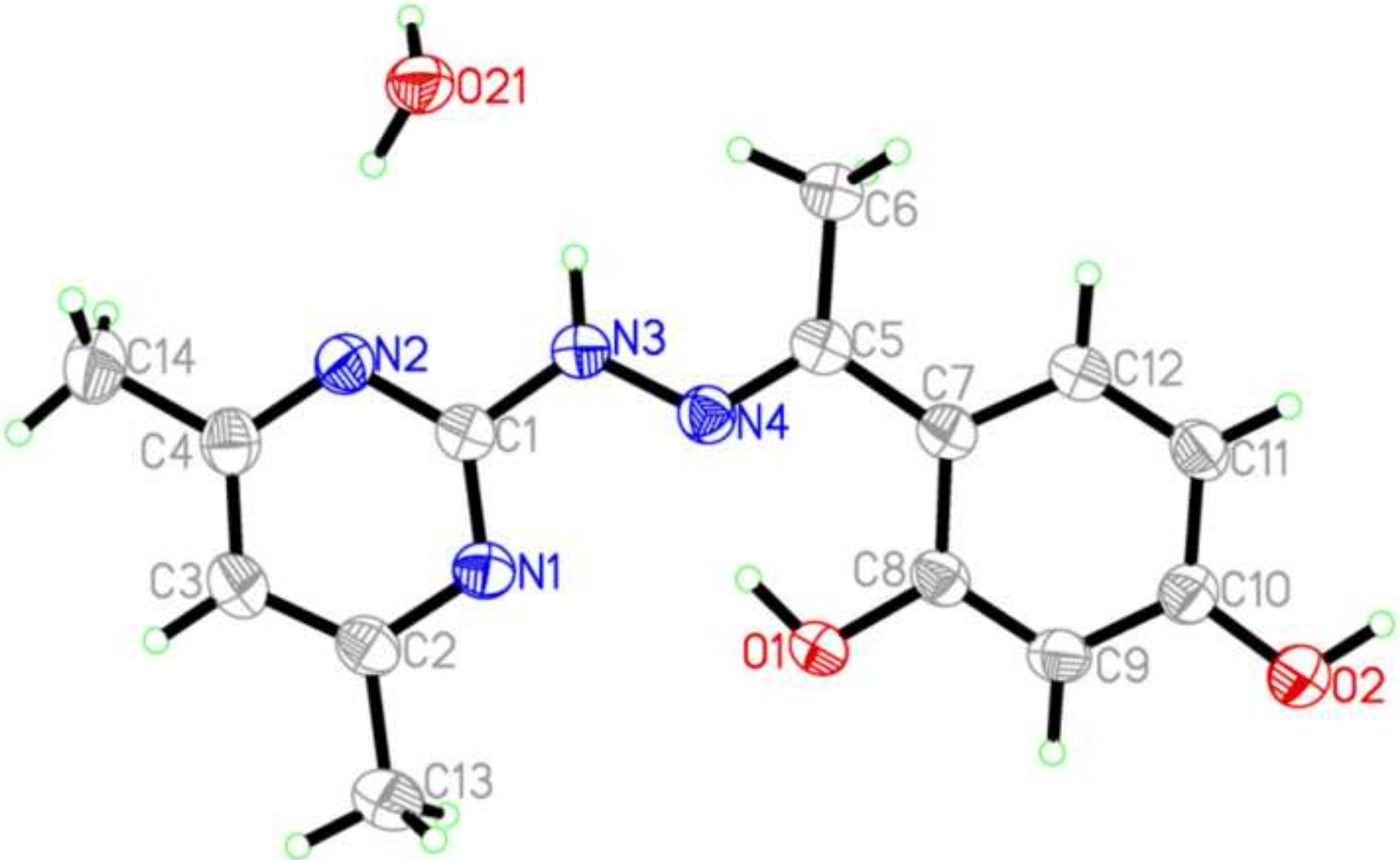

Figure 3

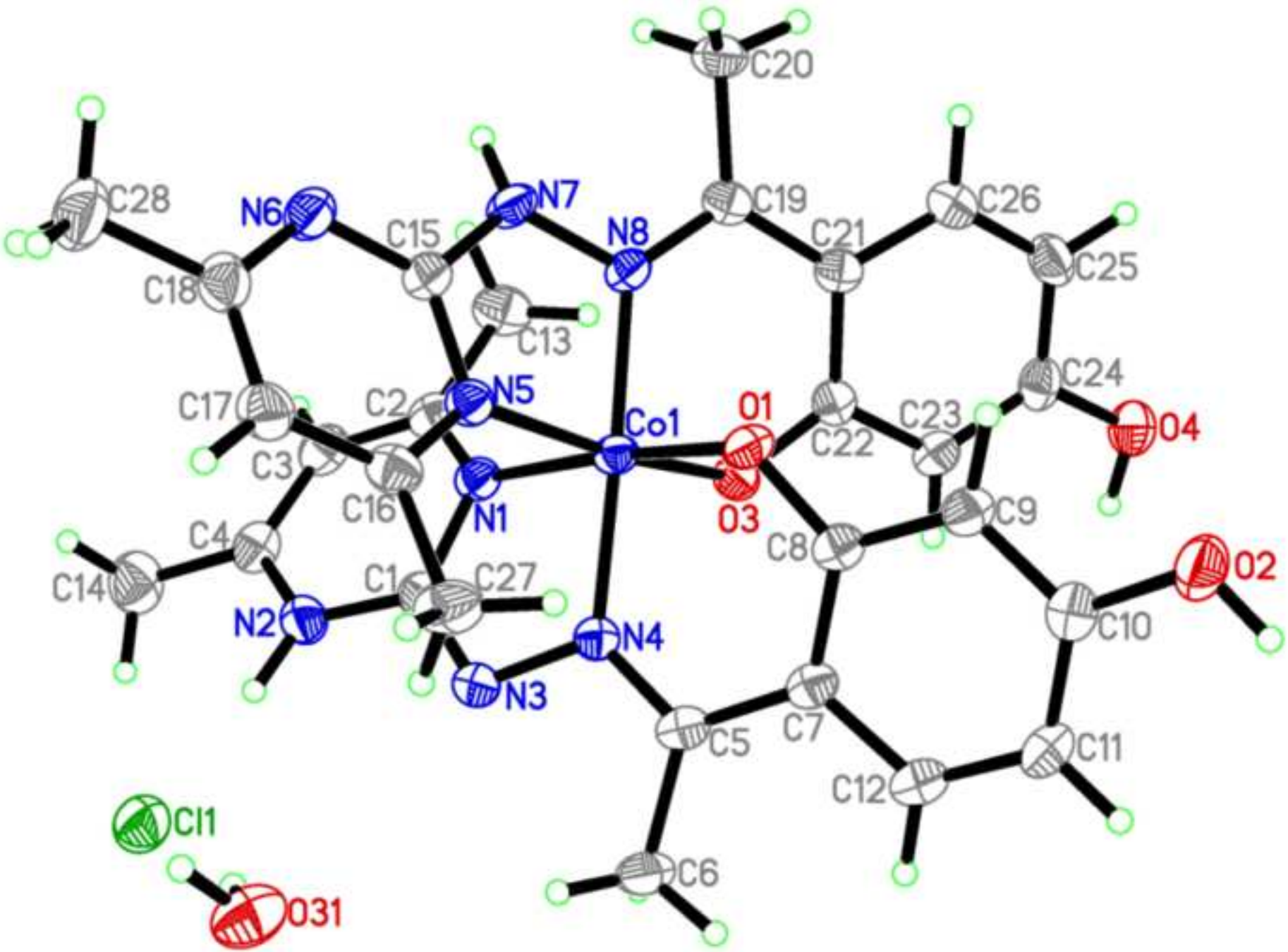

Figure 4

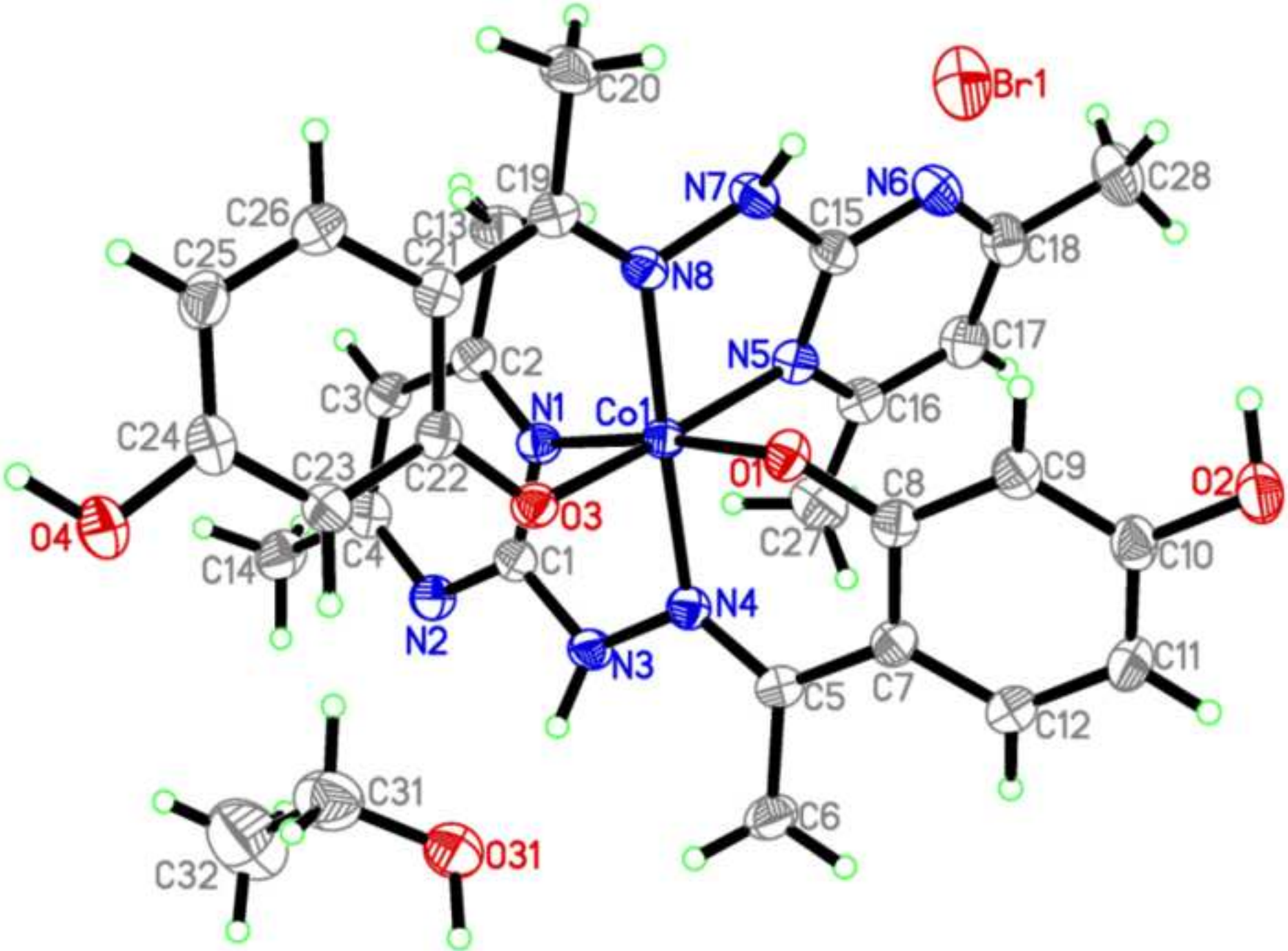

Figure 5

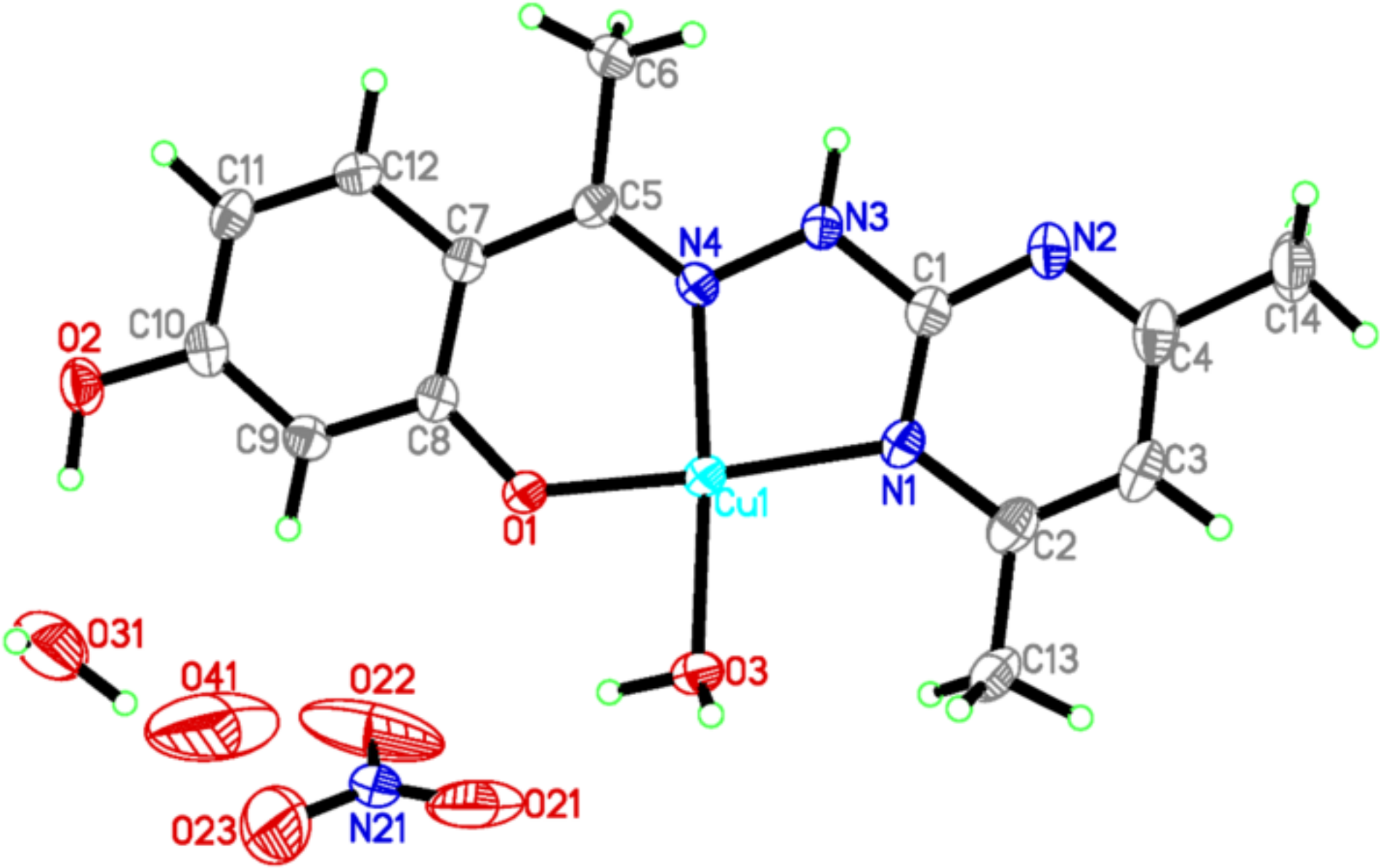

Figure 6

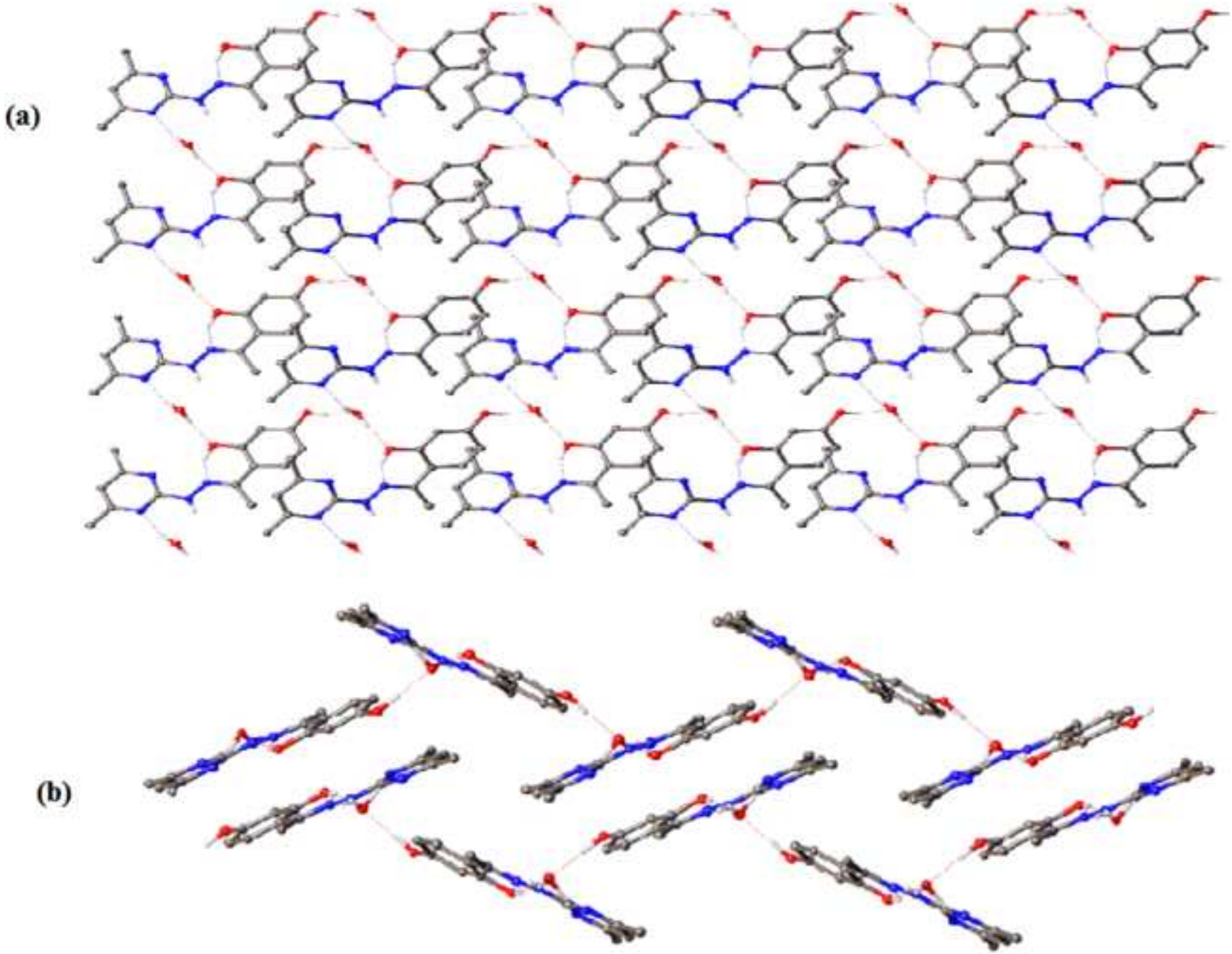

Figure 7

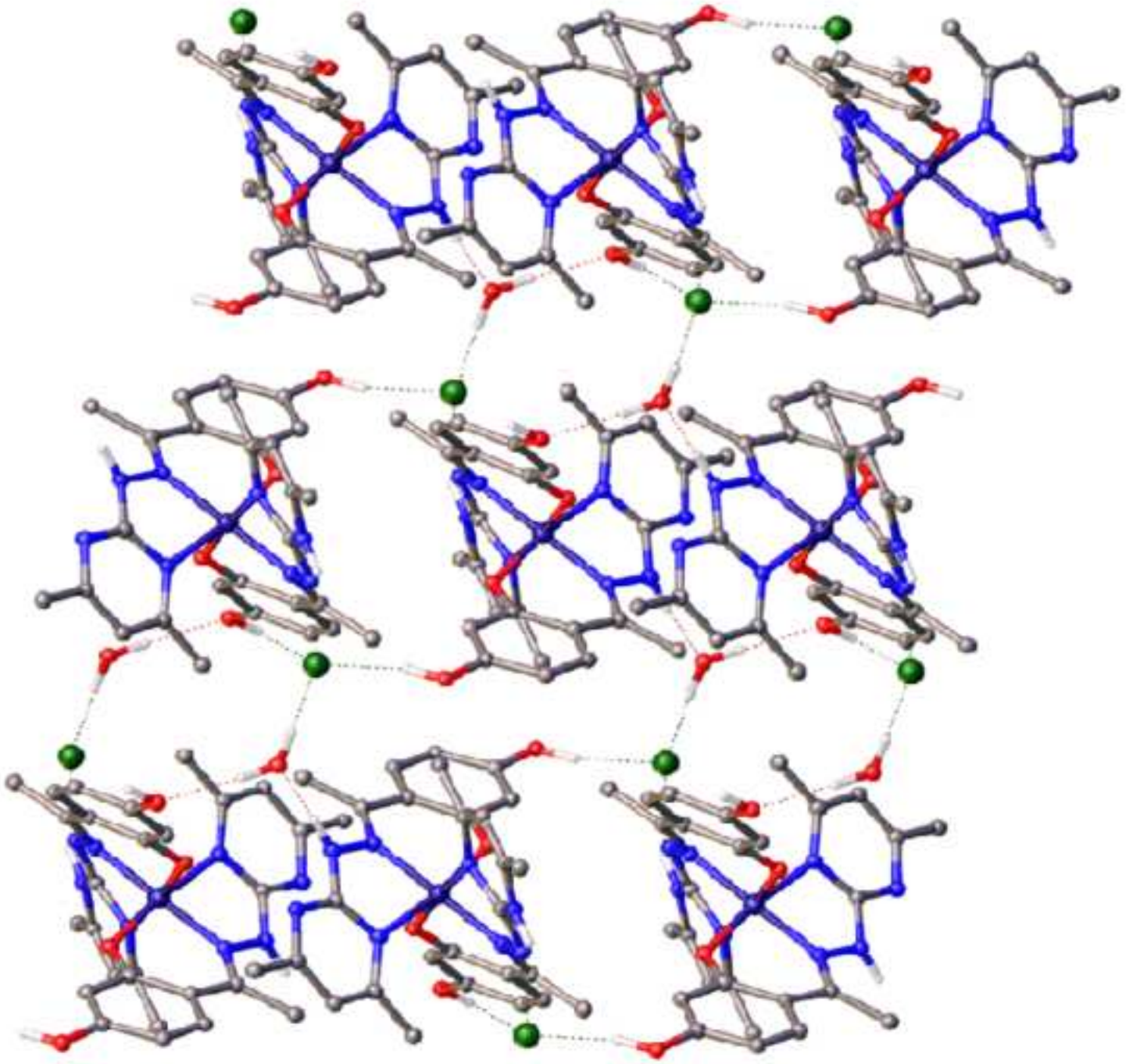

Figure 8

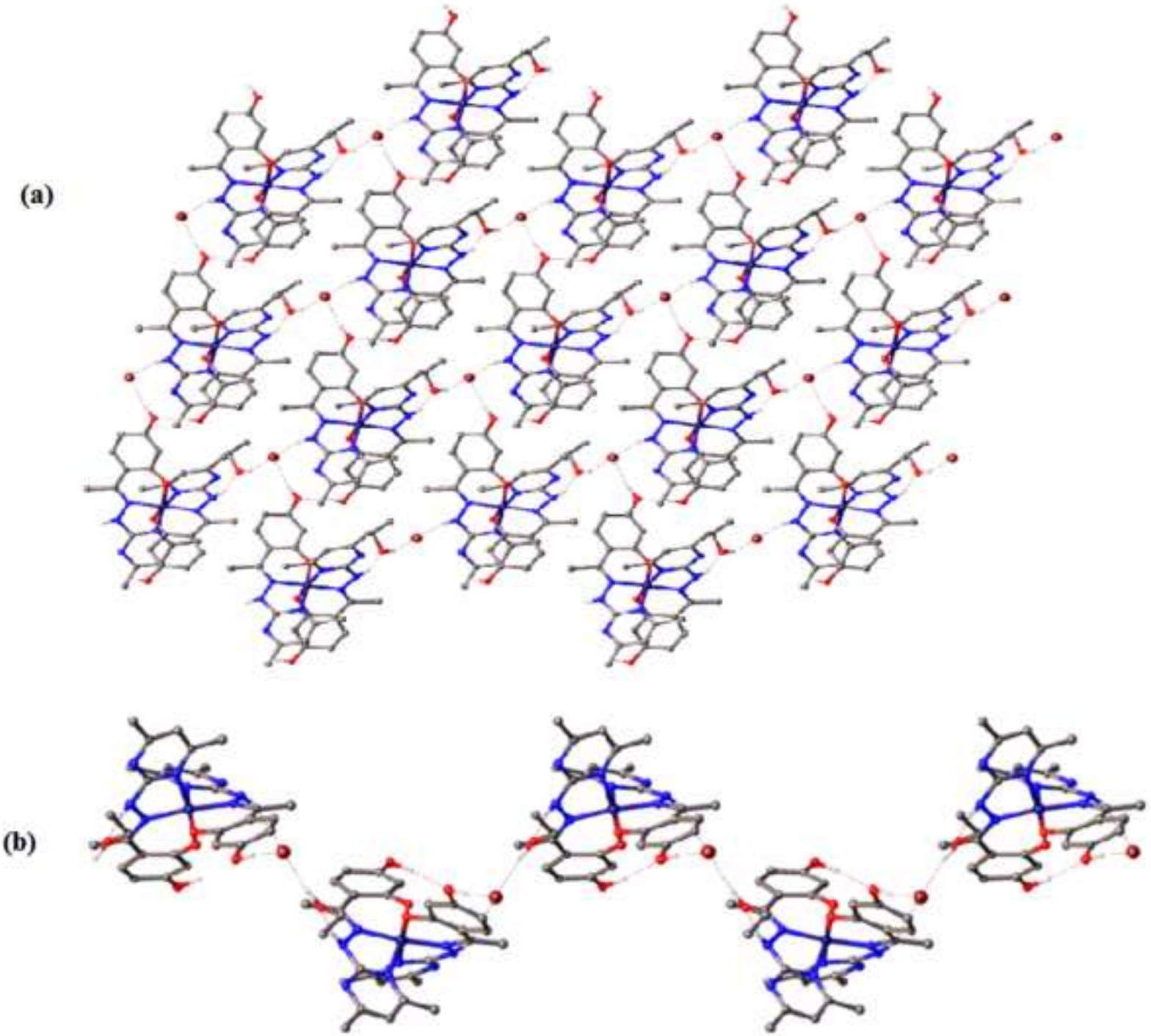

Figure 9

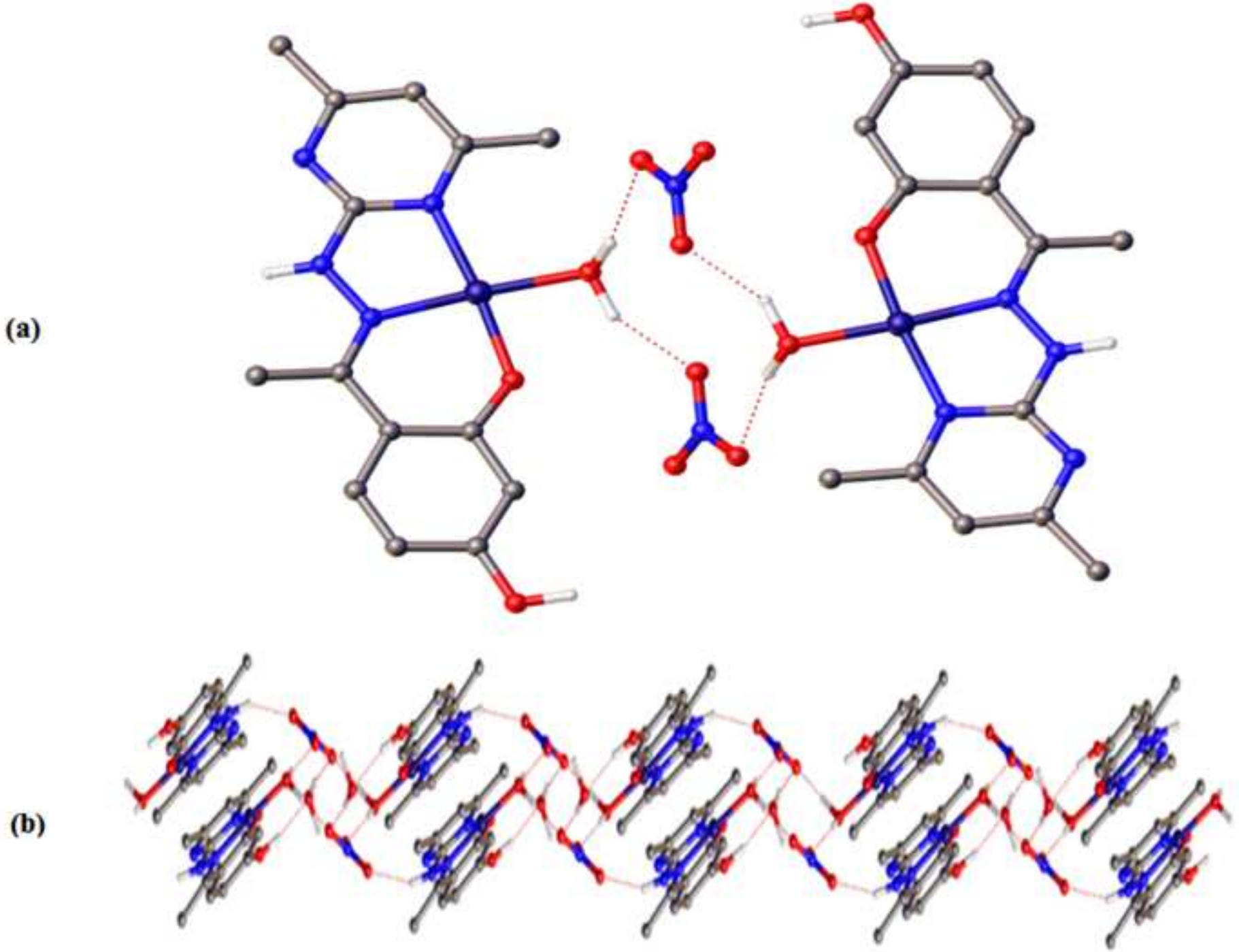

Figure 10

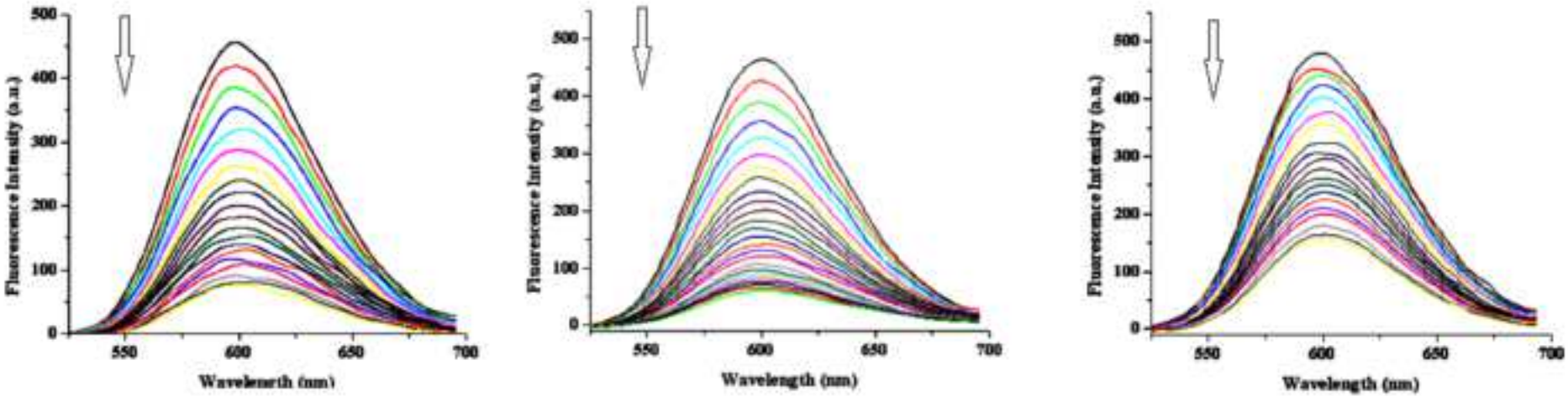

(a) (b) (c)

Figure 11

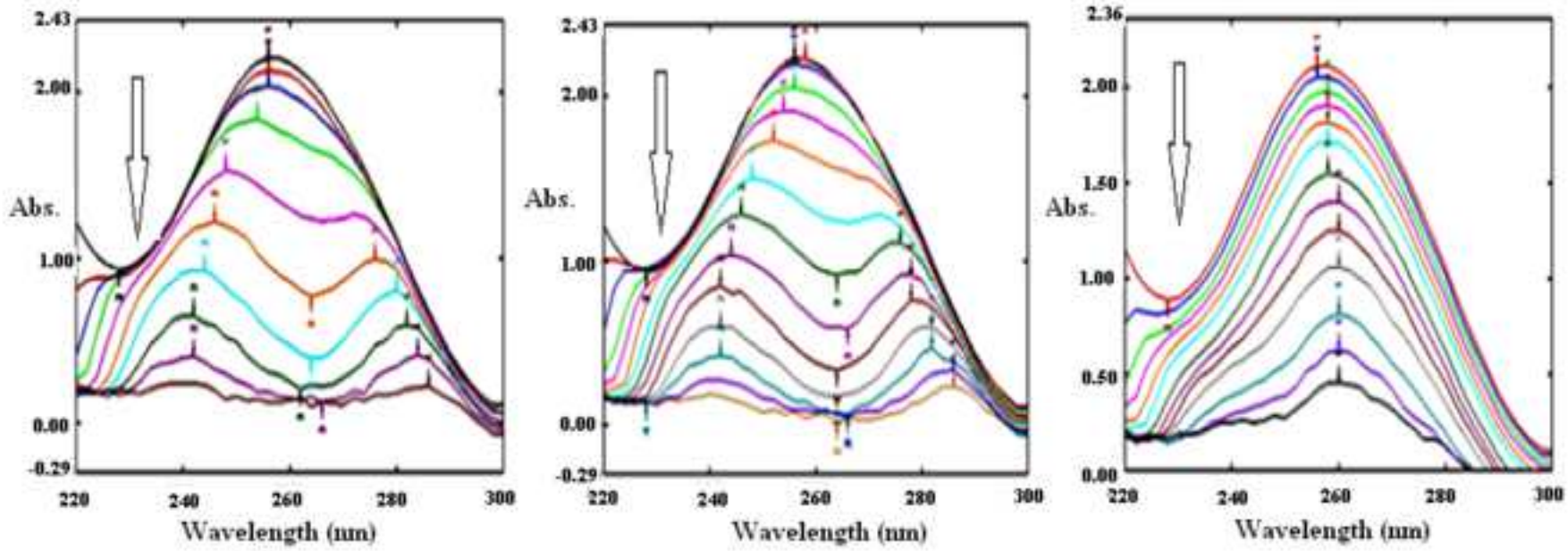

Figure 12

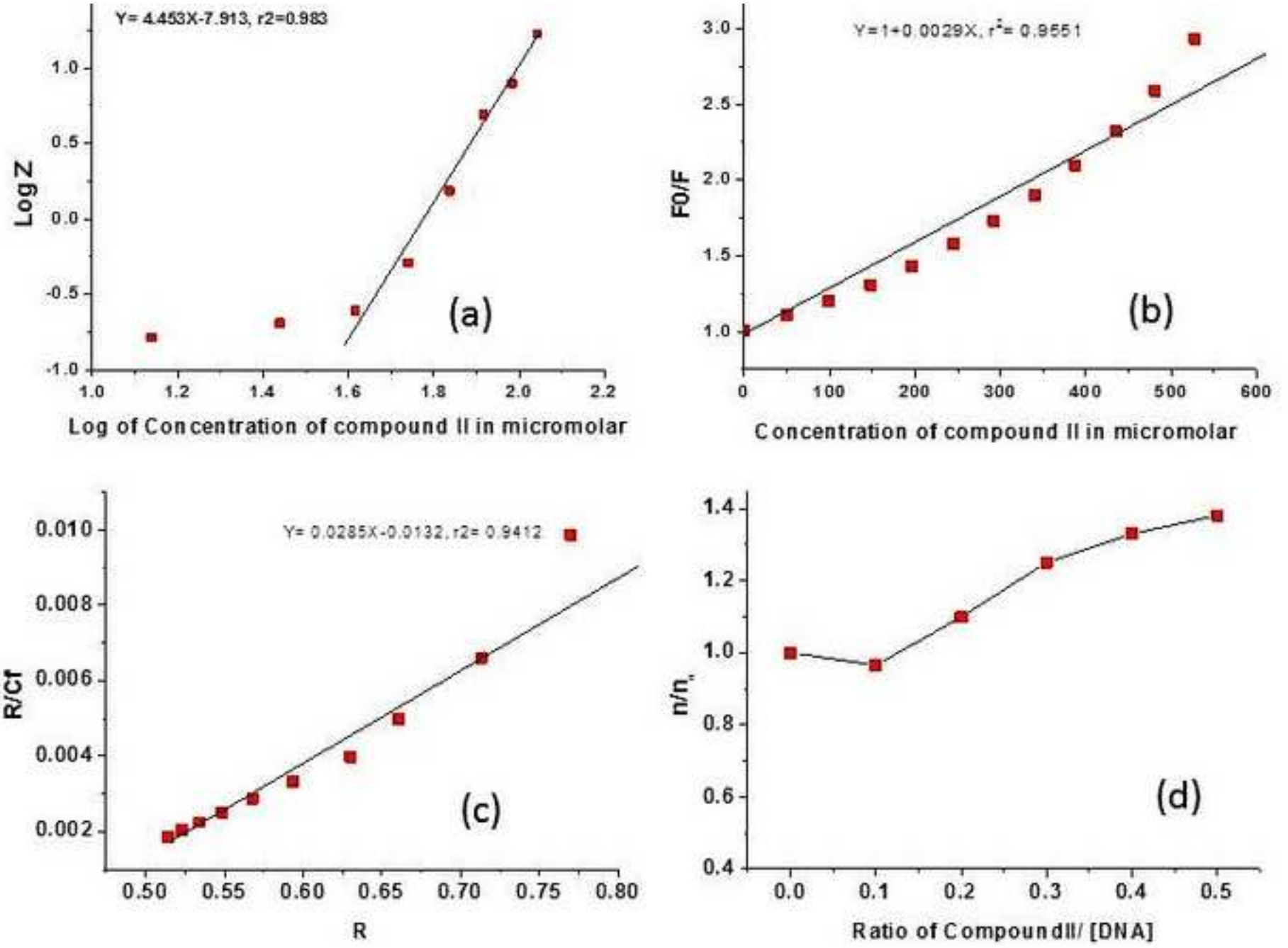

Figure 13

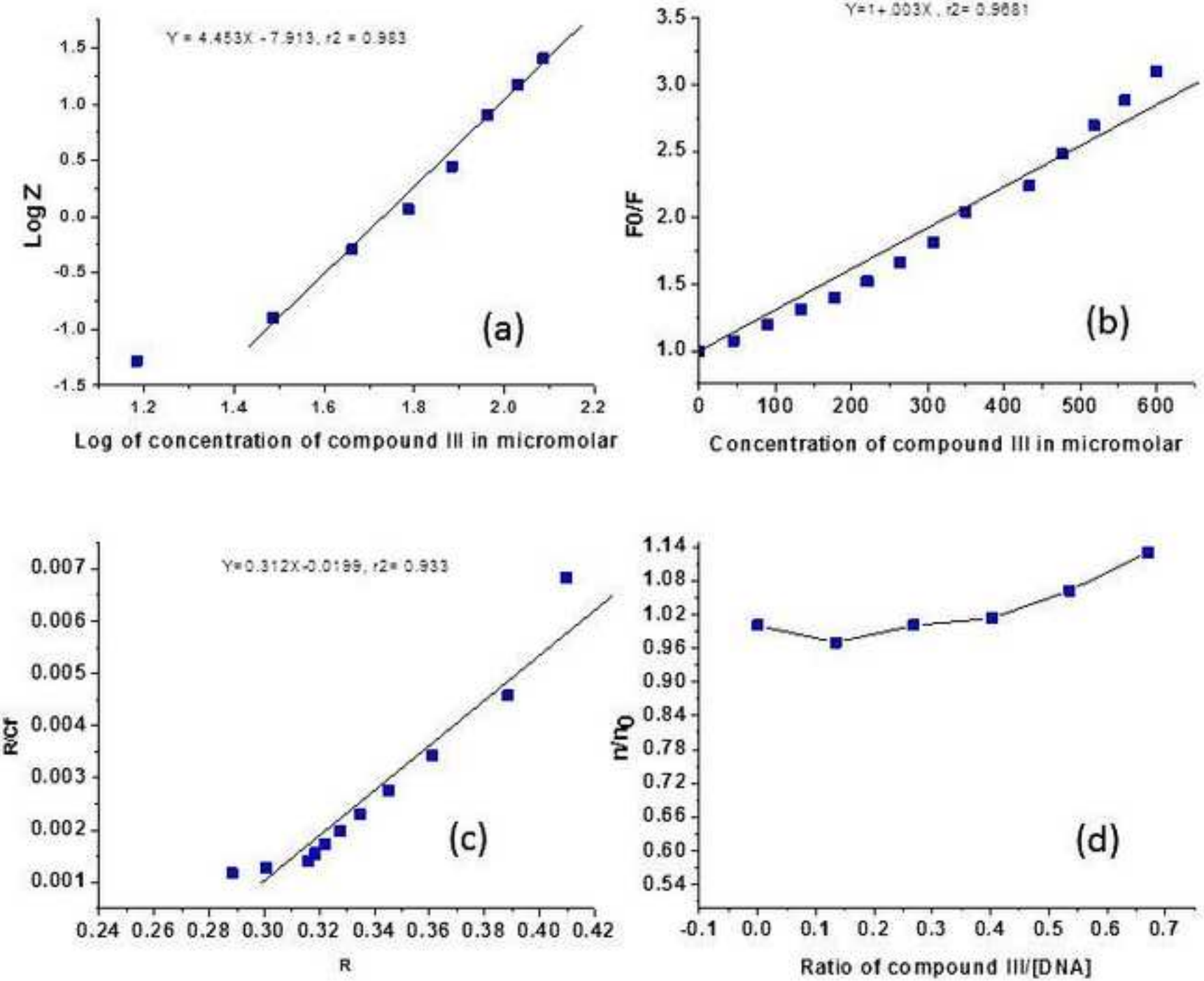

Figure 14

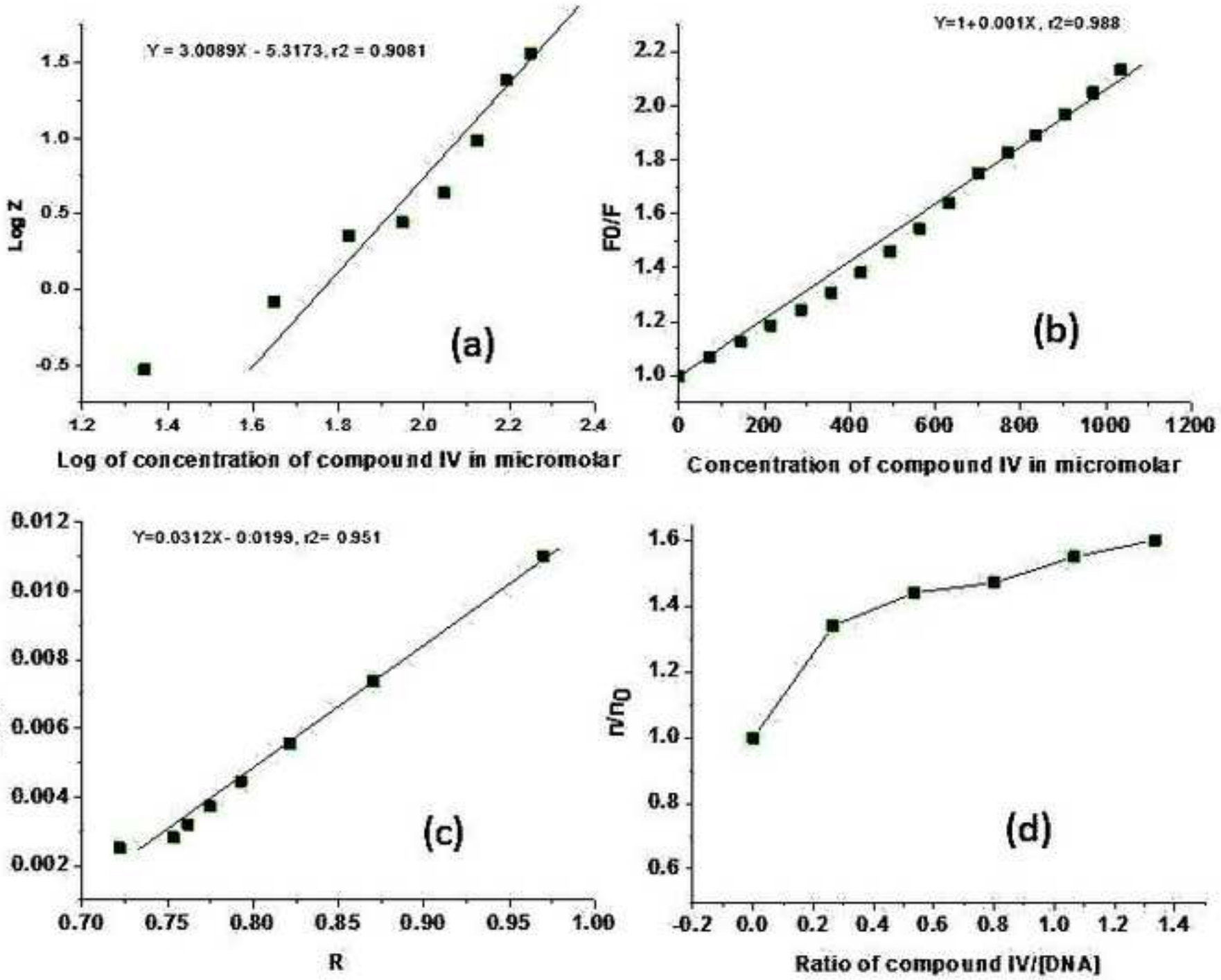

A new pyrimidine based Schiff base ligand and its Co(III) & Cu(II) complexes have been synthesized. The structural conformations of Co(III) and Cu(II) complexes have been established by X-ray studies and the detailed DNA binding activities and mode of DNA binding with metal complexes have been reported.

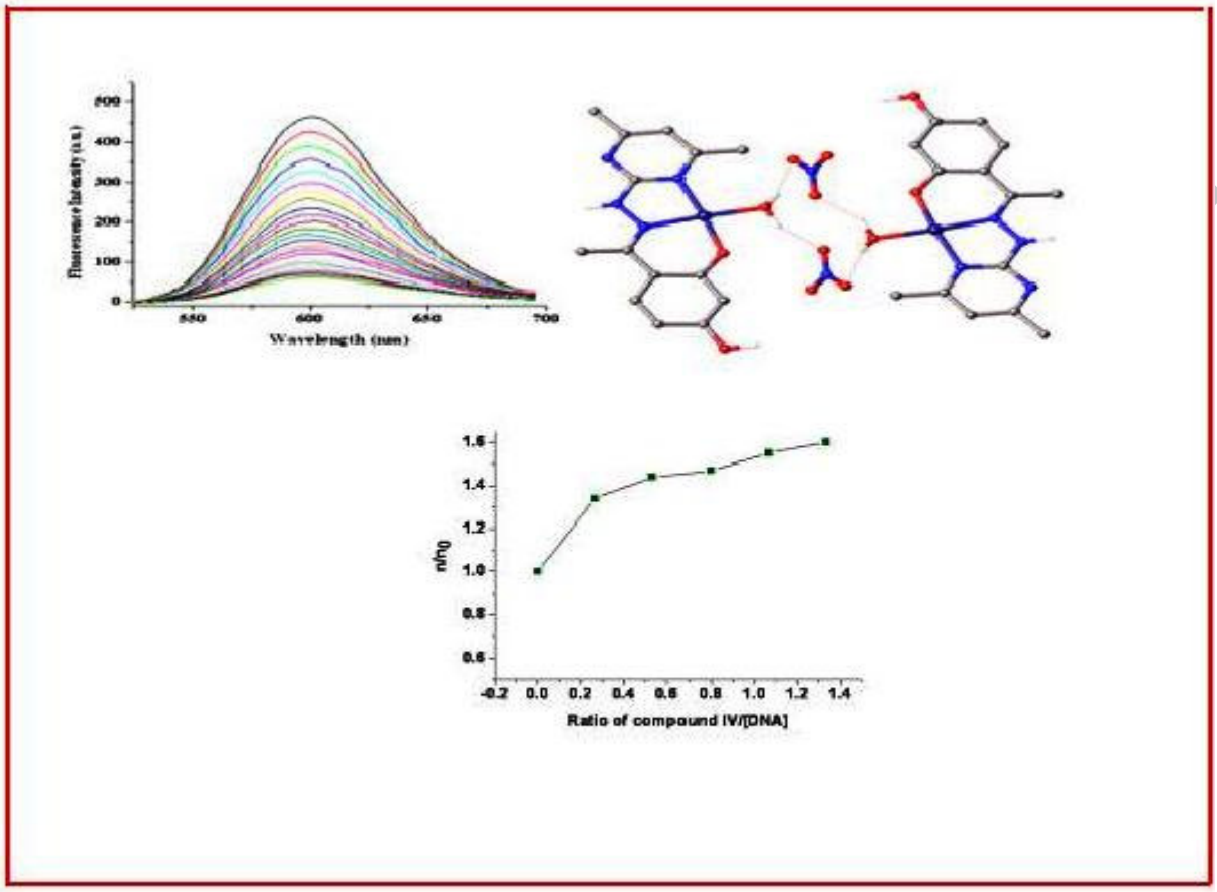

Highlights (for review)

Synthesis; X-ray crystallography; Hydrogen bonding interactions; DNA binding activities